

2 **Evaluating Residual Compressive strength of Post-fire Concrete using Raman**
3 **Spectroscopy**

4 *Tanya Kerr¹, Marleen Vetter², Jose Gonzalez-Rodriguez^{2,*}*

5
6 *1. Department of Physics, University of the West Indies, Kingston, Jamaica*

7 *2. School of Chemistry, University of Lincoln, Joseph Banks Laboratories, Green Lane, LN6 7DL, Lincoln,*
8 *UK, telephone: +441522886878, email:jgonzalezrodriguez@lincoln.ac.uk*

9
10
11 **ABSTRACT**

12 Cement and water within the concrete mass create a hydrated phase which acts as the glue for
13 holding the sand and coarse aggregates in place to develop a strong construction material. The
14 most important phase within the cement matrix is that of calcium silicate hydrate (CSH), which is
15 largely responsible for the concrete strength. Decomposition of the CSH phase due to high
16 temperatures will affect compressive strength of the concrete.

17 Raman bands at 1083, 709 and 276 cm^{-1} , which are representative of the CaCO_3 and CSH presence
18 in the concrete matrix phases can be used to assess changes in compressive strength as a result of
19 thermal decomposition. The ratio between 1083/709 cm^{-1} bands was calculated and correlated to
20 the compression strength of the concrete. The results show there is a rapid decline in strength
21 around a critical peak ratio of 8.78 and a residual compressive strength of 0.62, closely following
22 a polynomial curve. The tool developed here allows an indirect evaluation of the temperature the
23 concrete has been exposed to by studying the band.

24 A case study from a fire scene taken from a warehouse in Kingston (Jamaica) is also presented
25 with the conclusion and results compared. The study showed that Raman spectroscopy has the
26 potential to provide in-situ non-destructive testing of fire damaged concrete rapidly and accurately.

27
28 **Keywords:** Post-fire; concrete; Raman spectroscopy; compressive strength; CSH; elevated
29 temperature

32

33

34 1. Introduction

35 Concrete is a composite material made up of different ratio combinations of cement, sand, coarse
36 aggregates and water. Cement and water create a hydrated phase which acts as the glue for
37 holding the sand and coarse aggregates in place to develop a strong construction material [1].

38 The cement matrix consists of several phases, the most critical of which is the calcium silicate
39 hydrate (CSH), which is largely responsible for the concrete strength There are studies that
40 indicate that decomposition of the CSH phase would result in a reduction in compressive
41 strength of the concrete member[2–4].

42 Concrete structural stability is of great concern once a building has been exposed to elevated
43 temperatures resulting from a fire. Instability in structures are caused by the development of
44 voids and cracks resulting from thermal shock and decomposition of the hydrated cement
45 matrix[1,3]. This change in structural integrity is usually measured as a loss in compressive
46 strength[3,5].

47 Several studies have shown that there is a decrease in compressive strength associated with high
48 exposure temperatures[6–8]. TGA studies indicate that certain losses occur in the chemistry of
49 cement matrix at specific temperatures. Upon exposure to elevated temperatures CSH, which is
50 the main contributor to mechanical strength, decomposes. At about 350 °C there is the release of
51 chemically bound water. At 560 °C the decomposition of CSH increases drastically with
52 temperature[3,9]. As the concentration of CSH decreases in the solid concrete mass, the
53 compressive strength should decrease as the reduction in the hydrated phase causes shrinkage
54 affecting how tightly bound the aggregates are[10,11]. Work by Vetter et al. using Raman
55 spectroscopy demonstrated that this technique is a suitable tool to follow concrete chemistry

56 changes with increasing temperature exposure[9]. Furthermore, Hagar [5] showed that a decline
57 in residual compressive with increasing temperature is almost inevitable. Therefore, it should be
58 expected that a clear relationship between temperature, compressive strength and chemical
59 change exists. This is of great importance to assess the structural integrity of building after a fire.
60 Testing methods for assessing post fire concrete for loss in compressive strength are often
61 destructive and assess this variable based on either chemical or mechanical changes. TGA allows
62 for the assessment of concrete based on chemical changes, while other methods assess directly
63 based on mechanical changes, most of which are destructive techniques[3,12].
64 Raman spectroscopy is a technique used to identify and assess the chemical structure of
65 materials. Research done by Menendez [2] shows that the progression of damage to a concrete
66 wall is typically 5 cm into the surface. Therefore, Raman spectroscopy with the correct selection
67 of laser wavelength and penetration energy and distance could be an ideal tool for this purpose. It
68 is expected that from the spectrum of a concrete piece a relationship to the residual compressive
69 strength could be obtained.

70 The work developed in this manuscript is based on data generated for a typically used concrete
71 mix for residential structures after exposing them to different fire conditions. The residual
72 compressive strength for each selected scenario and the relationship to changes in Raman spectra
73 plotted was studied and correlations established. To the best of our knowledge this is the first
74 time Raman spectroscopy has been used to assess the physical structure of concrete subjected to
75 fire and offer an estimation of fire temperatures.

76 The work proposed here offers a non-destructive and portable method for assessing chemical
77 changes in concrete in the field that can be translated to mechanical variable, compressive

78 strength and to assess samples obtained from fire scenes and to establish a link to temperature
79 exposure.

80

81 2. **Materials and methods**

82 2.1 **Lab Tests**

83 2.1.1 **Sample Preparation - Concrete construction blocks**

84 Six-inch hollow blocks used for standard block and steel wall construction were purchased from
85 a local hardware. The blocks were filled as would be done in construction with Portland
86 pozzolan cement (Plus Carib Cement - Caribbean Cement Company Limited, Kingston,
87 Jamaica), washed natural sand (Primecrete by IAR, Kingston, Jamaica) and water (1:3:0.5). The
88 mortar used for filling the blocks was prepared by first placing water in a bucket, then the cement
89 was added and mixed at a slow speed for about 30 seconds using an electric mixer. The sand was
90 then gradually added over another 30 seconds period combining it at a slow mixing speed. This
91 was followed by mixing for an additional 30 seconds and then left to stand for 90 seconds, any
92 particles residing on the side of the bucket were quickly scrapped down. Finally, the mortar was
93 mixed one last time at a medium speed for 60 seconds. After filling the blocks, they were left to
94 dry over a 24-hour period.

95 The filled blocks were then cured in a water chamber at 26 °C for seven days to yield a
96 maximum strength of 12 MPa. Compression strengths were tested using a Humbolt 7515LE007
97 Compression Tester fitted with a RiceLine 720 controller (Test Mark Industries, Ohio, USA),
98 which had been calibrated by the Bureau of Standards of Jamaica.

99 2.1.2 **High temperature exposure**

100 The fire compartments used to simulate fire scenarios for assessment of concrete block were
101 modeled after Campbell [13]. The compartments were built using 2x4 treated lumber (3.8 x 8.9
102 cm) and drywall. The internal dimensions 0.91 x 0.91 x 0.61 m (LxWxH) with a drywall ceiling.
103 On side A as seen in figure 1, there was a ventilation opening with the dimensions of 20 x 30 cm.
104 The furniture frame was built using plywood of 15 cm thick, the furniture cushions were made
105 from 2.54 cm thick polyurethane foam covered with batting and upholstery fabric. The wood
106 furniture frame was reinforced with metal wires on the bottom or the back before covered in fabric.
107 The sofa, armchair and chair were 34 cm, 16 cm and 10 cm long respectively. The concrete blocks
108 to be tested were placed along the wall (side **B**) as in figure 1.

109



110

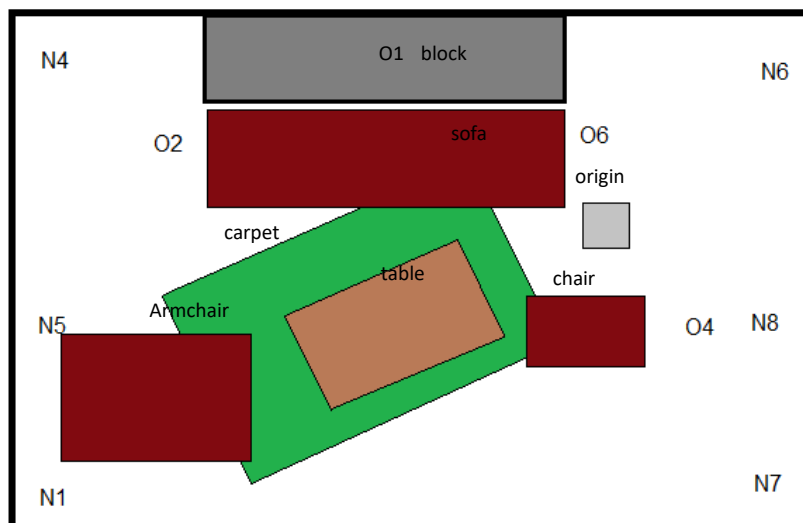
111 Figure 1: Showing a typical fire compartment design used for assessing concrete behaviour at
112 elevated temperatures. **A** – specifies the front of the compartment; **B** – specifies the rear of the
113 compartment

114

115 2.1.3 Design Fire

116 Different fire scenarios were implemented inside the compartment to expose the concrete blocks
117 to elevated temperatures of 500 °C, 560 °C, 605°C and 680 °C to achieve decomposition of the
118 cement matrix. These temperatures were selected as significant changes were expected based on
119 literature [5]. The position of the fire origin and the first material ignited was varied to change
120 the fire dynamics. A miniature wood crib with gasoline was introduced between the sofa and the
121 chair in the final compartment to achieve 680°C.

122 Different scenarios were considered in our study. The difference between scenarios was based on
123 the addition and removal of furniture pieces and the location of the starting point for the fire. The
124 details of each scenario are given in Table 1. Figure 2 below represents the typical layout of the
125 burn cell used in this study. Compartment temperature was collected using Omega Engineering
126 8-channel USB thermocouple data acquisition module TC-08 and Omega high temperature
127 Nextel insulated XC-20-K-168 K-type thermocouples. The data module was designated O and N
128 to differentiate between channel readings from the two modules as indicated in figure 2.



129

130 Figure 2: Shows the layout of a typical burn cell. O1 through to N8 represent the layout of the
131 thermocouples in the cell to collect temperature (O and N are identifiers for the datalogger used)

132
133
134
135
136
137

Table 1. Summary of the changes to the burn cell to yield different temperature profiles which were achieved to study concrete behaviour.

Scenarios	Fire origin
1	The origin was located between the sofa and the chair as a bin fire with rolled newspaper
2	The origin was situated at the front of the sofa, where the sofa was directly lit by a lighter
3	The fire was started in a wastepaper bin with rolled newspaper in front of doorway on the carpet and at the foot of the standard chair.
4	A wood crib soaked with gasoline was situated between the sofa and the chair.

138

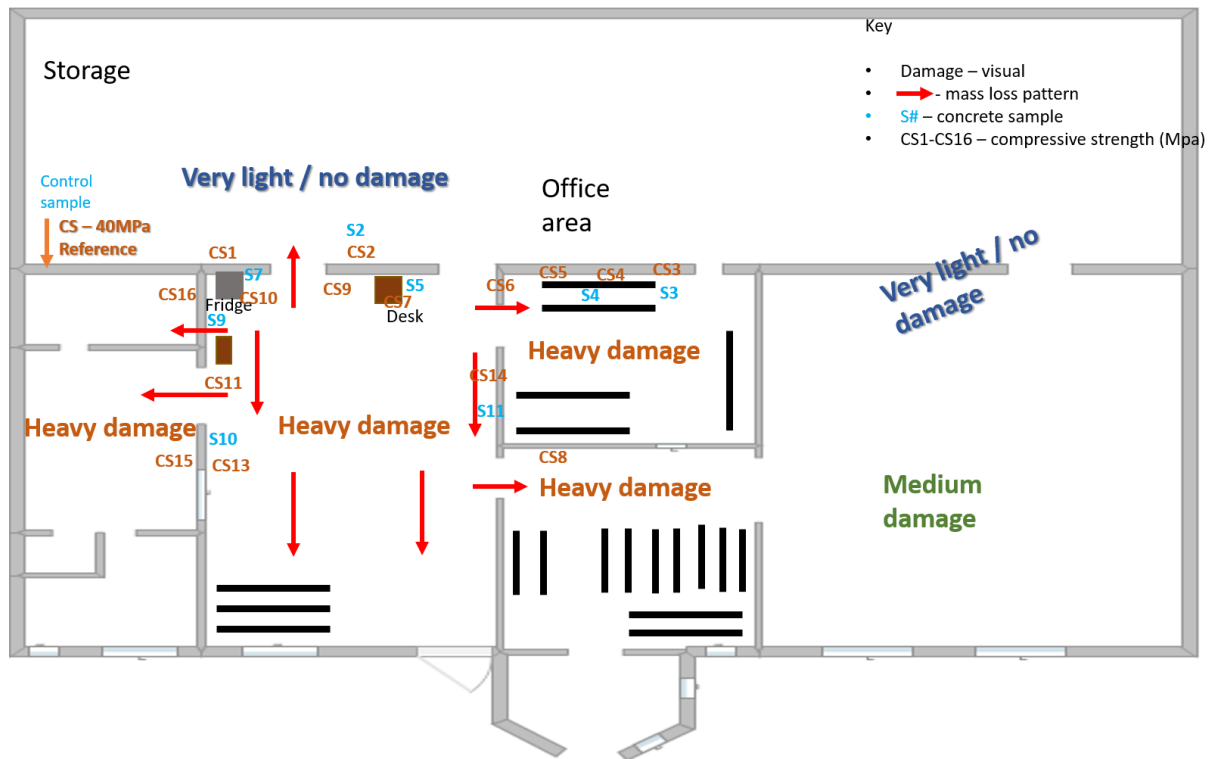
139 2.1.4 Sampling

140 The samples used in Raman testing were removed from the surface of the front face of the blocks
141 which had been exposed directly to the compartment fire. All samples were taken following the
142 compression tests. The samples from the concrete blocks were dusted to remove excess soot
143 from the surface, this was done to avoid obscuring the Raman spectrum of the concrete surface.

144 2.2 Field Test

145 A warehouse building constructed from prefabricated high strength concrete walls was used for
146 the field test. The structure experienced a fire five days prior to in situ testing and sample
147 collection. The building was laid out as seen in figure 3 below, where the assessment was carried
148 out across eight compartments.

149 An initial walk through was conducted to determine the order of testing and sampling. Test data
 150 and samples were collected from the area of least damage to the area of heaviest damage as
 151 recommended by the NFPA 921 Guide for Fire and Explosion Investigation. During the
 152 inspection an area was selected as a concrete reference point to represent the structural
 153 characteristics (compressive strength and spectral) prior to the fire.



154
 155 Figure 3. Shows the layout of the warehouse, onsite observations, and sampling sites. CS-denotes
 156 samples where compressive strength analyses were performed. S-denotes samples taken where
 157 spectra were performed.

158
 159 2.2.1 Data collection

160 A digital PROCEQ Type-L Co.SSO.5S SilverSchmidt PC N concrete test hammer was used to
 161 collect the compressive strength in the areas of interest. Prior to use in field the instrument was

162 tested against known samples to determine good working ability. In situ testing was carried out
163 for each of the areas in figure 3 marked CS (compressive strength). Each location was first
164 prepared by lightly grinding the surface with a grindstone to create a flat testing site. Then a 3 by
165 3 grid was drawn, and a rebound hammer reading taken in each grid to gather an average
166 estimate of the compressive strength. The individual and average values were logged by the
167 instrument and then later downloaded for analysis using the Hammerlink software from Proceq.
168 Compressive strength data was collected from sixteen sites moving from area of least to highest
169 damage based on a visual inspection.

170 Mass loss fire patterns were noted throughout the inspection and was documented by the red
171 arrows in figure 2. This is significant as it is a technique that can be used for tracking fire
172 movement and isolating the area of origin. This was done to determine how the proposed method
173 correlated with the patterns.

174 2.2.2 Sampling for Raman Analysis

175 Three of the nine grids were sampled from ten (10) of the sixteen compressive strength test sites.
176 Test sites that were in close proximity and had very similar compressive strengths were omitted
177 from the sample collection. Samples were collected on average as a 2 cm x 2 cm and a 1 cm
178 thickness, this depth contains the most significant damage [2].

179

180 2.3 Raman Spectroscopy analysis

181 Raman analyses were carried out on samples removed from the external surface of the blocks.
182 Surface samples were taken from both the unexposed and fire exposed concrete for comparison.
183 Spectra were collected using Horiba Jobin Yvon Labram Raman with an Olympus BX41

184 confocal microscope attachment. It was fitted with a 532 nm green laser from Laser Quantum
185 with a laser intensity ranging from 150-300 mW for analysis. The 20x objective was used for all
186 spectroscopy analysis. A 100 nm slit, 1600 gr/mm and a 1000 μm whole size were used
187 throughout and exposure time was usually between 10-30 seconds. To minimize the effects of
188 sample inhomogeneity, data was collected from multiple points (9) on each sample and averaged
189 to create a Raman profile for all concrete samples.

190 2.4 **Data Analysis**

191 Raman spectral comparisons between concrete at room temperature and those exposed to
192 different elevated temperatures were performed with Bio-Rad Know-it-all software.

193 Preprocessing include baseline correction and Savitsky–Golay seven-point smoothing [14]. The
194 data was then converted to a CSV file and Teraplot 3D software was used to visualize the Raman
195 spectra with reference to compressive strength.

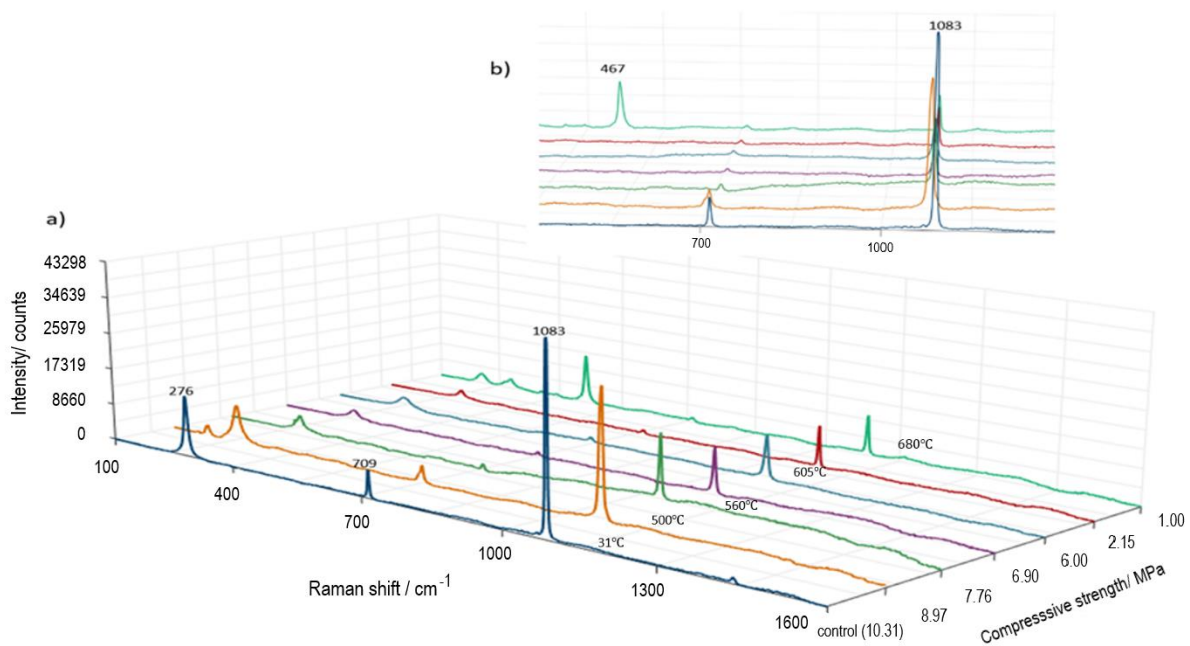
196 A plot of Raman peak ratio versus residual compressive strength was assembled to determine
197 correlation between the two factors. The standard error was calculated for peak ratios associated
198 with each change in compressive strength to determine significance of the work presented. Also,
199 a plot of temperature versus Raman peaks ratio was also conducted to assess the possibility of
200 post-fire temperature estimation.

201

202 3. **Results and discussion**

203 3.1 **Laboratory Study**

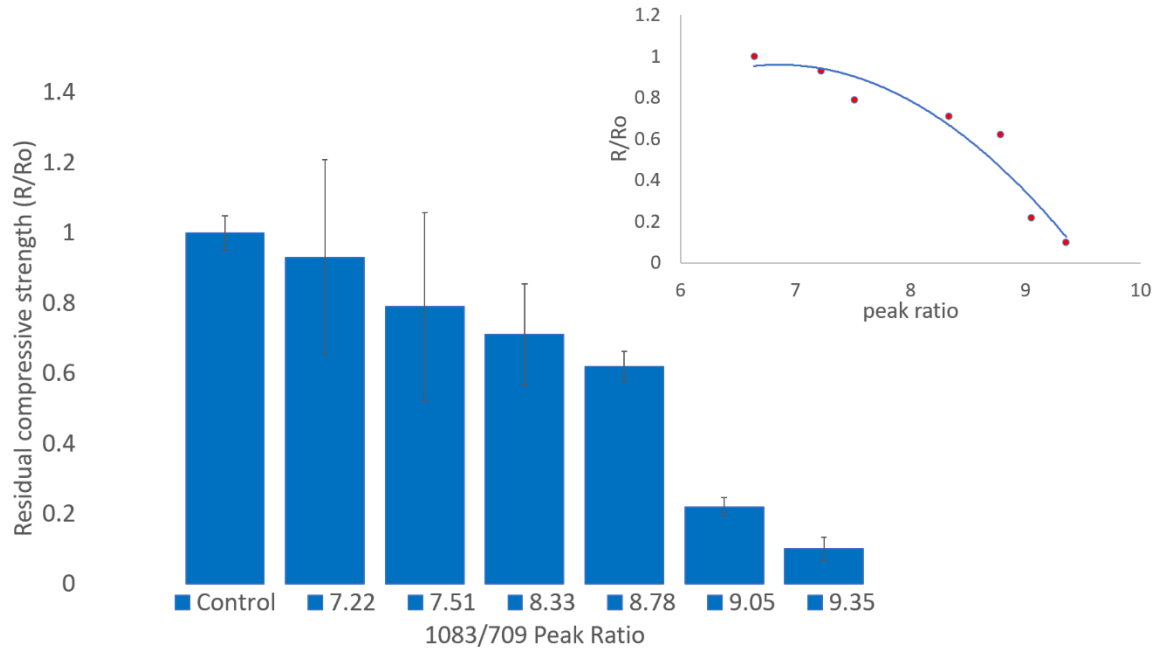
204 To assess the concept put forward in this paper on the use of a non-destructive spectral technique
 205 for determining changes in compressive strength due to decomposition of the CSH phase we
 206 exposed the concrete samples to the different scenarios described in section 2.1. The
 207 temperatures resulting from the test scenarios ranged from 500 °C to 680 °C as seen in figure 4.
 208 Figure 4 shows the average Raman spectrum for a concrete filled block and its corresponding
 209 compressive strength at room temperature (dark blue), along with the spectrum of several blocks
 210 which have been exposed to different high temperatures to achieve decomposition of the CSH
 211 phase.



212
 213 Figure 4. (a) Raman spectra of concrete with different compressive strengths and subjected to
 214 different temperatures to follow thermal degradation; (b) band shift with temperature and quartz
 215 phase 467 cm⁻¹.
 216 The dominant peaks from the surface of the concrete blocks were observed at 1083, 709 and 276
 217 cm⁻¹, which are representative of the CaCO₃ and CSH presence in the concrete matrix[15]. These

218 peaks which were seen to be sensitive to changes in temperature as recorded by Vetter et al[9],
219 now also demonstrated sensitivity to compressive strength as they changed due to matrix
220 decomposition. The control sample (dark blue) represents concrete that has not been exposed to a
221 harsh environment. The subsequent spectra show a reduction in each of these peaks with the
222 decline in compressive strength. In the inset for figure 4 (b), it can be seen that the Raman
223 spectrum experiences a peak shift particularly for both the peaks at 1083 cm^{-1} and more
224 significantly for 709 cm^{-1} peaks to higher wavenumbers with a broadening of the peaks at higher
225 temperature. These shifts are as a result of changes in the chemical environment of the cement
226 paste as Si-O bonds are broken and CaCO_3 increases [16]. This is significant as it suggests that
227 compressive strength changes can be tracked through these peaks. At low compressive strength
228 and higher temperature, the Raman spectrum showed the formation of a quartz phase indicated
229 by the 467 cm^{-1} peaks (Figure 3b).

230 To determine the usefulness of the Raman spectral data in assessing compressive strength, a plot
231 of the residual compressive strength (the ratio of the exposed concrete strength at different
232 temperatures to the room temperature compressive strength) was plotted against the 1083 to 709
233 cm^{-1} peak ratio in figure 5. The $1083/709$ peak ratio was calculated using the peak intensities
234 found in the Raman spectra corresponding to the four different scenarios.



235

236 Figure 5. Variation of residual compressive strength with Raman spectral changes and the
 237 standard error associated (n=4) with the Raman data collected for each concrete block

238 This ratio was used as they have shown significant changes with respect to changing

239 compressive strength and in order to standardize the obtained data. The residual compressive

240 strength gives the remaining compressive strength of the block following high temperature

241 exposure. The data in figure 5 showed minimal losses in strength with small changes in

242 compressive strength. There is a relatively constant decline in strength with the decrease in the

243 CSH peak ratio, however, there seems to be a critical peak ratio where there is rapid decline in

244 strength beyond that point. This is significant as this ratio can be an indicator for danger. In this

245 study the peak ratio at 8.78, which would correspond to a value of 0.62 in residual compressive

246 strength, is marking a critical point. This result is also in keeping with the study carried out by

247 Tantawy [17], where a gradual decline in compressive strength with increasing temperature

248 could be observed. This study also showed that at the critical temperature of 450 °C there is a

249 rapid decline in strength. In our work the decline follows well a polynomial curve, as seen in

250 figure 5, with a relationship given by the equation $R/R_o = -0.0188(P1/P2)^2 - 0.0027(P1/P2) +$

251 1.0104 and having an R^2 value of 0.97. In a very recent study published in 2021, similar results
252 were observed by Alcaino et al [18] who assessed different concrete samples subjected to fire
253 and established ranges of non-destructive test variations according with safety criterion based on
254 strength variation. In their study, not involving spectroscopic methods, they established a danger
255 area for residual compressive strength of <0.60 , which is in perfect agreement with our
256 conclusions.

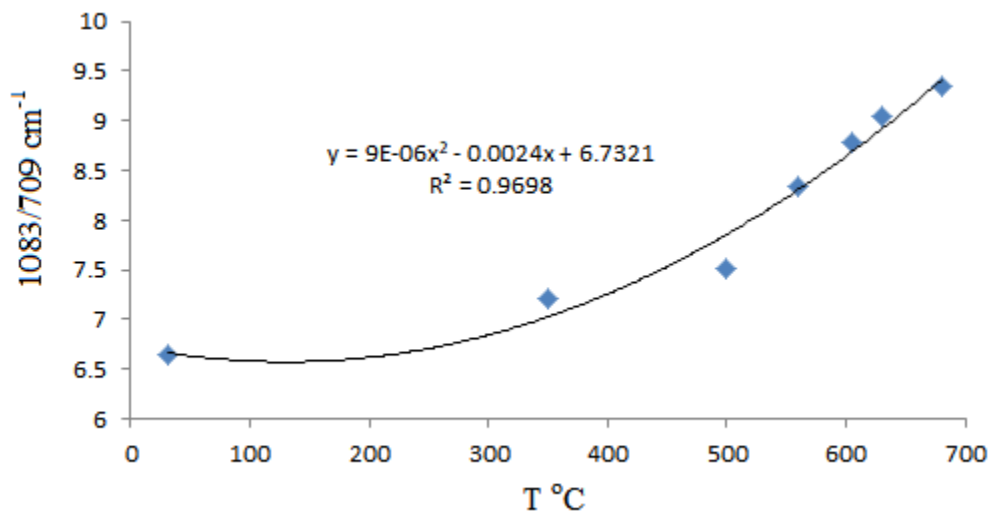
257 The error associated with using the selected marker for assessing changes in residual
258 compressive strength was also evaluated. The data seen in figure 5 supports the choice of using
259 the 1083/709 marker as the error associated with this peak ratio for control sample concrete
260 showed marginal differences with a standard deviation of 0.12. The error analysis also indicated
261 that there are small changes in the phases in concrete at relatively low temperatures and the
262 higher end of the residual compressive strength. The plot shows that a significant difference in
263 phase can be detected by Raman spectroscopy for larger losses in compressive strength. The
264 standard error data also implies that Raman spectroscopy will provide not only a specific ratio
265 for a mix design that indicates fit or not fit for purpose results, but it does so more accurately
266 where there is critical loss.

267 Previous studies performed by the authors have established that Raman spectra can be used to
268 track the changes in the CSH phase due to exposure to elevated temperatures, which now alludes
269 to the use of Raman spectroscopy for tracking temperature history and compressive strength loss.

270 This method opens the door to the possibility of using Raman as a valid tool to assess concrete
271 strength. A larger study with several typical mix designs should be done to generate a calibration
272 chart with a concrete control and concrete exposed to elevated temperatures to validate the
273 method for use in fire analysis and civil engineering. The collection of more data would allow

274 for the development of a model for determining the residual compressive strength of a structural
275 member post fire. The practical field application would entail analysis of the unexposed side of
276 the wall as a reference to determine 1083/709 ratio and then the relative loss from the fire
277 exposed side of the wall using portable Raman spectrometers. A study done by Menendez and
278 Vega [2] demonstrated that fire damage is most often limited to a few centimeters from the
279 surface despite prolonged exposure to high temperatures such as 500 °C. This may then allow the
280 rear side of the wall to be taken as a reference.

281 The next practical application of the use of Raman peak ratios, as described before, would be the
282 estimation of the temperature at which that section of concrete has been subjected to. Figure 6
283 shows a plot of the temperature used in our controlled experiments versus the Raman peaks ratio.
284 We obtained a good fit to a quadratic equation with a low error and a good correlation coefficient
285 ($R^2=0.9698$)



286

287 Figure 6. Relationship between Raman 1083/709 cm⁻¹ band ratio and temperature collected for
288 each concrete block.

289

290

291 3.2 Case study

292 The usability of the laboratory method in a real practical scenario was performed using Raman
293 data obtained from the building structure described in section 2.2. Samples from areas where
294 heavy damage produced by fire was observed were taken to calculate their band ratios and assess
295 their compressive strength and estimate the fire temperature. Table 2 shows a summary of the
296 findings for the different areas as shown in figure 3.

297

298

299

Table 2. Summary of data collected from field test and samples collected

Test site	CS (MPa)	Residual compressive strength (Mpa)	Samples collected	1083/709	Estimated Temperature (°C)
Control	40	1.00	Control	7.65	-
CS1	22	0.55	S1	8.15	552.1
CS2	28	0.70	S2	9.22	675.7
CS3	34	0.85	S3	8.77	626.5
CS5	27	<u>0.68</u>	S4	<u>9.44</u>	697.8
CS7	25	0.63	S5	8.26	566.4
CS9	18	0.45	S6	8.33	566.2
CS10	20	<u>0.50</u>	S7	<u>12.01</u>	910.6
CS11	16	<u>0.40</u>	S8	<u>10.54</u>	797.3
CS12	20	<u>0.50</u>	S9	<u>11.93</u>	904.9
CS14	14	<u>0.35</u>	S11	No 709	-
CS16	15	<u>0.38</u>	S10	No 709	-

300

301 From the results of table 2 we can establish that, based on the Raman peak ratios, any test site
302 area with a Raman band ratio above 8.78, should be considered unsafe (underlined on table 2).

303 This generally correlates well with the safety value below 0.6 for residual compressive strength
304 determined by Alcaino at al [18], which reinforces the validity of the spectral analysis. There

305 were two points for CS14 and CS16 for which no band at 709cm^{-1} could be calculated, although
306 in principle, this should already indicate that the phase transition has been so intense that the
307 concrete structural integrity is already severely compromised -as indicated by the low
308 compressive strength. Following the model established in Figure 6, we could also calculate an
309 approximation of the temperature of the fire. In this sense, the estimated values calculated agree
310 with the severe damage observed for some areas and the danger zones previously established. It
311 also agreed with the bracket of temperatures and estimations made by fire investigators on the
312 scene after the fire. We need to be careful when using this estimation as it only indicates the
313 temperature at which the phase transition of the difference phases in the concrete occurred and
314 not an indication of the maximum temperature reached in the fire. In order to estimate the
315 maximum temperature of the fire, we would need to include the time variable and perform other
316 experiments which were not the aim of this study.

317

318 Conclusions

319 The research conducted has proven some of the original hypotheses. Raman spectroscopy can
320 track chemical changes in concrete, as evidenced from previous published work, but also can be
321 used to assess a mechanical variable, residual compressive strength, and to assess samples
322 obtained from fire scenes and to establish a link to temperature exposure. Raman spectroscopy
323 can be used to offer an estimate temperature and to determine concrete behavior as a result of
324 high temperature exposure without destructive testing. The results have demonstrated that
325 Raman bands at 1083 and 709 cm^{-1} , which are representative of the CaCO_3 and CSH presence in
326 the concrete matrix phases can be applied to assess changes in residual compressive strength as a
327 result of thermal decomposition. Using the $1083/709$ ratio the residual strength we can offer an

328 idea of the deterioration of the concrete strength through the residual compressive strength. Our
329 study showed that there is a critical peak ratio of 8.78 beyond which there has been rapid loss in
330 strength deemed dangerous. This is significant, as this ratio could be utilized as a safety
331 indicator. Also, the estimated temperatures obtained by the model were within the estimations
332 given by fire investigators. The data shows good potential which should be further extended to
333 carefully define the application of this technique. Portable Raman spectroscopy has the potential
334 to provide accurate in situ non-destructive testing of fire damaged concrete in a non-destructive
335 and fast way given the portability of this technique.

336

337 References

- 338 [1] K. Krzemień, I. Hager, Post-fire assessment of mechanical properties of concrete with the
339 use of the impact-echo method, *Constr. Build. Mater.* (2015).
340 doi:10.1016/j.conbuildmat.2015.08.007.
- 341 [2] E. Menendez, L. Vega, Analysis of the behaviour of the structural concrete after the fire at
342 the Windsor Building in Madrid, *Fire Mater.* (2010) 95–107. doi:10.1002/fam.
- 343 [3] O. Arioz, Effects of elevated temperatures on properties of concrete, *Fire Saf. J.* 42 (2007)
344 516–522. doi:10.1016/j.firesaf.2007.01.003.
- 345 [4] G.F. Peng, S.Y.N. Chan, M. Anson, Chemical kinetics of C-S-H decomposition in
346 hardened cement paste subjected to elevated temperatures up to 800°C, *Adv. Cem. Res.*
347 (2001). doi:10.1680/adcr.2001.13.2.47.
- 348 [5] I. Hager, Behaviour of cement concrete at high temperature, (2018). doi:10.2478/bpasts-

- 349 2013-0013.
- 350 [6] B. Georgali, P.E. Tsakiridis, Microstructure of fire-damaged concrete. A case study, *Cem.*
351 *Concr. Compos.* 27 (2005) 255–259. doi:10.1016/j.cemconcomp.2004.02.022.
- 352 [7] K. Sakr, E. El-Hakim, Effect of high temperature or fire on heavy weight concrete
353 properties, *Cem. Concr. Res.* (2005). doi:10.1016/j.cemconres.2004.05.023.
- 354 [8] K. Akçaözöğlü, Microstructural examination of concrete exposed to elevated temperature
355 by using plane polarized transmitted light method, *Constr. Build. Mater.* 48 (2013) 772–
356 779. doi:10.1016/j.conbuildmat.2013.06.059.
- 357 [9] M. Vetter, J. Gonzalez-Rodriguez, E. Nauha, T. Kerr, The use of Raman spectroscopy to
358 monitor phase changes in concrete following high temperature exposure, *Constr. Build.*
359 *Mater.* (2019). doi:10.1016/j.conbuildmat.2019.01.165.
- 360 [10] E. Annerel, L. Taerwe, Revealing the temperature history in concrete after fire exposure
361 by microscopic analysis, *Cem. Concr. Res.* 39 (2009) 1239–1249.
362 doi:10.1016/j.cemconres.2009.08.017.
- 363 [11] U.K. Ahmad, C.K. Voon, Detection of Accelerants in Fire Debris using Headspace Solid
364 Phase Microextraction-Capillary Gas Chromatography, *Malaysian J. Anal. Sci.* 7 (2001)
365 57–63.
- 366 [12] N. Ukrainczyk, M. Ukrainczyk, J. Sipusic, T. Matusinovic, XRD and TGA Investigation
367 of Hardened Cement Paste, 11. *Conf. Mater. Process. Frict. Wear MATRIB'06, Vela*
368 *Luka.* (2006) 22–24.
- 369 [13] M. Campbell, REDUCED SCALE ENCLOSURE TESTING WITH LOW HEAT

370 RELEASE INITIAL FUEL PACKAGES, in: Proc. 7th Int. Symp. Fire Investig. Sci.
371 Technol., Symposium on Fire Investigation Science and Technology, 2014.

372 [14] A.G. Ioan Tomuta, Alina Porfire, Tibor Casian, Multivariate calibration for the
373 development of vibrational spectroscopic methods, in: M. Stauffer (Ed.), Calibration
374 Valid. Anal. Methods A Sampl. Curr. Approaches, First, IntechOpen, London, 2018: pp.
375 35–60.

376 [15] R.J. Kirkpartick, J.L. Yarger, P.F. McMillan, P. Yu, X. Cong, Raman spectroscopy of C-
377 S-H, tobermorite, and jennite, *Adv. Cem. Based Mater.* 5 (1997) 93–99.
378 doi:10.1016/S1065-7355(97)00001-1.

379 [16] N. Garg, Raman spectroscopy for characterizing and determining the pozzolanic reactivity
380 of fly ashes, (2012) 151.

381 [17] M.A. Tantawy, Effect of High Temperatures on the Microstructure of Cement Paste, *J.*
382 *Mater. Sci. Chem. Eng.* (2017) 33–48. doi:10.4236/msce.2017.511004.

383 [18] P. Alcaíno, H. Santa-María, C. Magna-Verdugo, L. López. Experimental fast-assessment of
384 post-fire residual strength of reinforced concrete frame buildings based on non-destructive
385 tests. *Constr. Build. Mater.* 234, 117371. doi.org/10.1016/j.conbuildmat.2019.117371

386

387

388